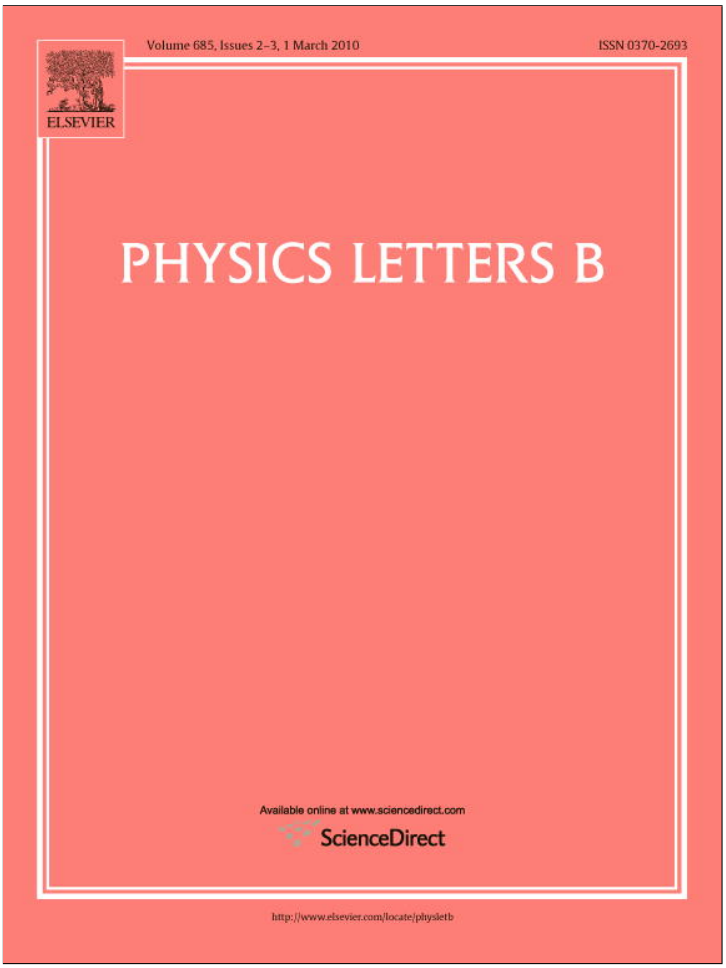

Physics Letters B 685 (2010) 134–140

Contents lists available at ScienceDirect

Physics Letters B

www.elsevier.com/locate/physletb

Measurement of $\Gamma_{ee}(J/\psi)\cdot\mathcal{B}(J/\psi\to e^+e^-)$ and $\Gamma_{ee}(J/\psi)\cdot\mathcal{B}(J/\psi\to\mu^+\mu^-)$

V.V. Anashin [a], V.M. Aulchenko [a,b], E.M. Baldin [a,b,*], A.K. Barladyan [a], A.Yu. Barnyakov [a], M.Yu. Barnyakov [a], S.E. Baru [a,b], I.V. Bedny [a], O.L. Beloborodova [a,b], A.E. Blinov [a], V.E. Blinov [a,c], A.V. Bobrov [a], V.S. Bobrovnikov [a], A.V. Bogomyagkov [a,b], A.E. Bondar [a,b], D.V. Bondarev [a], A.R. Buzykaev [a], S.I. Eidelman [a,b], Yu.M. Glukhovchenko [a], V.V. Gulevich [a], D.V. Gusev [a], S.E. Karnaev [a], G.V. Karpov [a], S.V. Karpov [a], T.A. Kharlamova [a,b], V.A. Kiselev [a], S.A. Kononov [a,b], K.Yu. Kotov [a], E.A. Kravchenko [a,b], V.F. Kulikov [a,b], G.Ya. Kurkin [a,c], E.A. Kuper [a,b], E.B. Levichev [a,c], D.A. Maksimov [a], V.M. Malyshev [a], A.L. Maslennikov [a], A.S. Medvedko [a,b], O.I. Meshkov [a,b], S.I. Mishnev [a], I.I. Morozov [a,b], N.Yu. Muchnoi [a,b], V.V. Neufeld [a], S.A. Nikitin [a], I.B. Nikolaev [a,b], I.N. Okunev [a], A.P. Onuchin [a,c], S.B. Oreshkin [a], I.O. Orlov [a,b], A.A. Osipov [a], S.V. Peleganchuk [a], S.G. Pivovarov [a,c], P.A. Piminov [a], V.V. Petrov [a], A.O. Poluektov [a], I.N. Popkov [a], V.G. Prisekin [a], A.A. Ruban [a], V.K. Sandyrev [a], G.A. Savinov [a], A.G. Shamov [a], D.N. Shatilov [a], B.A. Shwartz [a,b], E.A. Simonov [a], S.V. Sinyatkin [a], Yu.I. Skovpen [a,b], A.N. Skrinsky [a], V.V. Smaluk [a,b], A.V. Sokolov [a], A.M. Sukharev [a], E.V. Starostina [a,b], A.A. Talyshev [a,b], V.A. Tayursky [a], V.I. Telnov [a,b], Yu.A. Tikhonov [a,b], K.Yu. Todyshev [a,b], G.M. Tumaikin [a], Yu.V. Usov [a], A.I. Vorobiov [a], A.N. Yushkov [a], V.N. Zhilich [a], V.V. Zhulanov [a,b], A.N. Zhuravlev [a,b]

[a] *Budker Institute of Nuclear Physics, 11, akademika Lavrentieva prospect, Novosibirsk, 630090, Russia*
[b] *Novosibirsk State University, 2, Pirogova street, Novosibirsk, 630090, Russia*
[c] *Novosibirsk State Technical University, 20, Karl Marx prospect, Novosibirsk, 630092, Russia*

ARTICLE INFO

Article history:
Received 9 December 2009
Received in revised form 18 January 2010
Accepted 22 January 2010
Available online 28 January 2010
Editor: M. Doser

Keywords:
J/ψ meson
Leptonic width
Full width
Leptonic universality

ABSTRACT

The products of the electron width of the J/ψ meson and the branching fraction of its decays to the lepton pairs were measured using data from the KEDR experiment at the VEPP-4M electron–positron collider. The results are

$$\Gamma_{ee}\times\Gamma_{ee}/\Gamma = 0.3323\pm 0.0064(\text{stat.})\pm 0.0048(\text{syst.})\ \text{keV},$$

$$\Gamma_{ee}\times\Gamma_{\mu\mu}/\Gamma = 0.3318\pm 0.0052(\text{stat.})\pm 0.0063(\text{syst.})\ \text{keV}.$$

Their combinations

$$\Gamma_{ee}\times(\Gamma_{ee}+\Gamma_{\mu\mu})/\Gamma = 0.6641\pm 0.0082(\text{stat.})\pm 0.0100(\text{syst.})\ \text{keV},$$

$$\Gamma_{ee}/\Gamma_{\mu\mu} = 1.002\pm 0.021(\text{stat.})\pm 0.013(\text{syst.})$$

can be used to improve the accuracy of the leptonic and full widths and test leptonic universality. Assuming $e\mu$ universality and using the world average value of the lepton branching fraction, we also determine the leptonic $\Gamma_{\ell\ell}=5.59\pm 0.12$ keV and total $\Gamma = 94.1\pm 2.7$ keV widths of the J/ψ meson.

1. Introduction

The J/ψ meson is frequently referred to as a hydrogen atom for QCD. The electron widths Γ_{ee} of charmonium states are rather well predicted by potential models [1,2]. The accuracy in the QCD lattice calculations of Γ_{ee} gradually approaches the experimental errors [3]. The total and leptonic widths of a hadronic resonance, Γ and $\Gamma_{\ell\ell}$, describe fundamental properties of the strong potential [4].

In this Letter we report a measurement of the product of the electron width and the branching fraction to an e^+e^- pair for

* Corresponding author.
E-mail address: E.M.Baldin@inp.nsk.su (E.M. Baldin).

0370-2693/$ – see front matter
doi:10.1016/j.physletb.2010.01.057

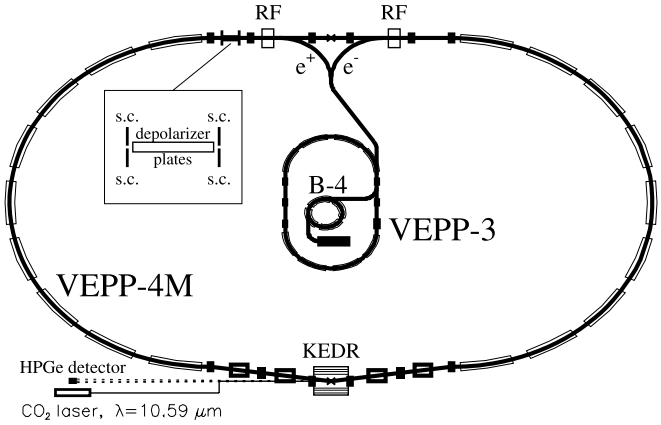

Fig. 1. VEPP-4M/KEDR complex with the resonant depolarization and the infrared light Compton backscattering facilities.

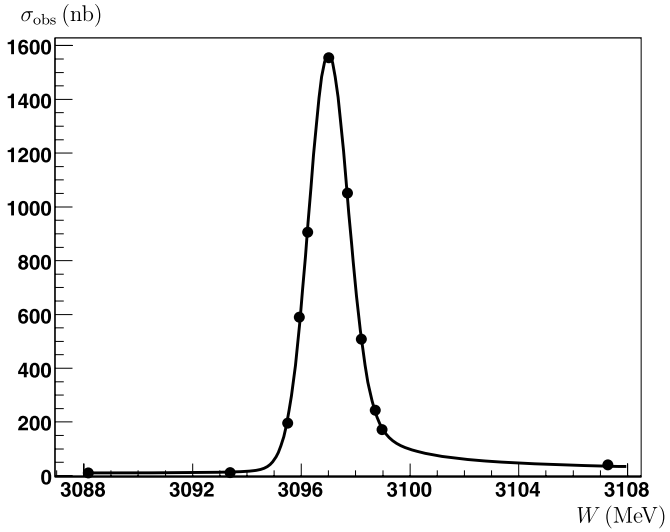

Fig. 2. Observed cross section of $e^+e^- \to$ hadrons in the J/ψ scan.

the J/ψ meson, $\Gamma_{ee} \times \Gamma_{ee}/\Gamma$. An experimental determination of $\Gamma_{ee} \times \Gamma_{ee}/\Gamma$ requires scanning the beam energy and measuring the cross section. In contrast to a measurement of the leptonic width itself, in this case knowledge of the efficiency for hadronic decays does not contribute to the final uncertainty. The problem considered can be reduced to measuring the area under the resonance curve for the process $e^+e^- \to J/\psi \to e^+e^-$. Additionally we have measured the product of the electron width of the J/ψ meson and the probability of its decay to the $\mu^+\mu^-$ pair, $\Gamma_{ee} \times \Gamma_{\mu\mu}/\Gamma$. Given independent data on the branching fraction $\mathcal{B}_{ee}$ [5], we use this result to evaluate the leptonic $\Gamma_{\ell\ell}$ and total Γ widths.

2. VEPP-4M collider and KEDR detector

The VEPP-4M collider [6] can operate in the broad range of beam energies from 1 to 6 GeV (see Fig. 1). The peak luminosity in the J/ψ energy range is about 2×10^{30} cm^{-2} s^{-1}.

One of the main features of the VEPP-4M is a possibility of precise energy determination. The resonant depolarization method [7,8] was implemented at VEPP-4 at the very beginning of experiments in early eighties for the measurements of the J/ψ and $\psi(2S)$ mass with the OLYA [9] detector and Υ family mass with the MD-1 [9] detector.

At VEPP-4M the accuracy of energy calibration with the resonant depolarization is improved to about 10^{-6}. Between calibrations the energy interpolation in the J/ψ energy range has the accuracy of 6×10^{-6} ($\simeq 10$ keV) [10].

To monitor beam energy during data taking the infrared light Compton backscattering is employed (with 50–70 keV precision in the J/ψ region), which was first developed at the BESSY-I and BESSY-II synchrotron radiation sources [11,12].

The KEDR detector [13] includes the vertex detector, the drift chamber, the scintillation time-of-flight counters, the aerogel Cherenkov counters, the barrel liquid krypton calorimeter, the endcap CsI calorimeter, and the muon system built in the yoke of a superconducting coil generating a field of 0.65 T. The detector also includes a tagging system to detect scattered electrons and study two-photon processes. The on-line luminosity is measured by two independent single bremsstrahlung monitors.

3. Experiment description

A data sample used for this analysis comprises 230 nb^{-1} collected at 11 energy points in the J/ψ energy range. This corresponds to approximately 15 000 $J/\psi \to e^+e^-$ decays. During this scan, 26 calibrations of the beam energy have been done using resonant depolarization.

The primary trigger signal was provided by a coincidence of two non-adjacent scintillation counters or an energy deposition in the endcap calorimeter of at least 100 MeV. A veto from the endcap-calorimeter crystals closest to the beam line was used to suppress the machine background.

The secondary trigger required at least two tracks in the drift chamber or at least one track and an energy deposition in the calorimeter of at least 70 MeV and the coincidence of two non-adjacent scintillation counters.

The hardware triggers use the analogous output of the calorimeter with reduced energy resolution. During the offline analysis real and simulated events pass through the software event filter which recalculates the trigger decision using a digitized response of the detector subsystems. The calorimeter energy thresholds in the event filter are toughened by a factor of 1.5 with respect to the instrumental values, suppressing the uncertainty in the latter and their possible instability.

Single bremsstrahlung and $e^+e^- \to e^+e^-$ events at polar angles in the range between 18° and 31° (the endcap calorimeter) were used in the relative measurement of luminosity. In order to evaluate $\Gamma_{ee} \times \Gamma_{ee}/\Gamma$, it was unnecessary to measure the absolute luminosity. Since $e^+e^- \to e^+e^-$ events analyzed here include both events of the resonance and a well-known non-resonant QED background, it is possible to perform an absolute calibration of the luminosity along with the derivation of $\Gamma_{ee} \times \Gamma_{ee}/\Gamma$.

Fig. 2 shows the observed cross sections of $e^+e^- \to$ hadrons in the J/ψ energy range. These data were used to fix the resonance peak position and to determine the beam energy spread. The value of the J/ψ mass agrees with the earlier VEPP-4M/KEDR experiments [10]. The accuracy of the energy spread was about 2%, including variations associated with the beam current.

4. Theoretical $e^+e^- \to \ell^+\ell^-$ cross section

The analytical expressions for the cross section of the process $e^+e^- \to \ell^+\ell^-$ with radiative corrections taken into account in the soft photon approximation were first derived by Ya.A. Azimov et al. in 1975 [14]. With some up-today modifications one obtains in the vicinity of a narrow resonance

$$\left(\frac{d\sigma}{d\Omega}\right)^{ee\to\mu\mu} \approx \left(\frac{d\sigma}{d\Omega}\right)^{ee\to\mu\mu}_{\rm QED} + \frac{3}{4M^2}(1+\delta_{\rm sf})\left(1+\cos^2\theta\right) \times \left\{\frac{3\Gamma_{ee}\Gamma_{\mu\mu}}{\Gamma M}\,\mathrm{Im}\,\mathcal{F} - \frac{2\alpha\sqrt{\Gamma_{ee}\Gamma_{\mu\mu}}}{M}\,\mathrm{Re}\,\frac{\mathcal{F}}{1-\Pi_0}\right\} \tag{1}$$

where a correction $\delta_{\rm sf}$ follows from the structure function approach of [15]:

$$\delta_{\rm sf} = \frac{3}{4}\beta + \frac{\alpha}{\pi}\left(\frac{\pi^2}{3} - \frac{1}{2}\right) + \beta^2\left(\frac{37}{96} - \frac{\pi^2}{12} - \frac{1}{36}\ln\frac{W}{m_e}\right) \tag{2}$$

and

$$\mathcal{F} = \frac{\pi\beta}{\sin\pi\beta}\left(\frac{M/2}{-W+M-i\Gamma/2}\right)^{1-\beta} \tag{3}$$

with

$$\beta = \frac{4\alpha}{\pi}\left(\ln\frac{W}{m_e} - \frac{1}{2}\right). \tag{4}$$

Here W is the center-of-mass energy and Π_0 represents the vacuum polarization operator with the resonance contribution excluded. The terms proportional to $\mathrm{Im}\,\mathcal{F}$ and $\mathrm{Re}\,\mathcal{F}$ describe the contribution of the resonance and the interference effect, respectively. The definition of leptonic width in Eqs. (1)–(4) implicitly includes vacuum polarization as recommended by PDG: $\Gamma_{\ell\ell} = \Gamma^0_{\ell\ell}/|1-\Pi_0|^2$, where Γ^0_{ee} is the lowest-order QED value.

The function $\mathcal{F}$ in Eq. (3) appears from the integration (see [16], where one can also find the definition of $\mathcal{F}$ for the relativistic Breit–Wigner amplitude) and differs from that in Ref. [14] by the $\pi\beta/\sin\pi\beta$ factor.

For the e^+e^- final state one has

$$\left(\frac{d\sigma}{d\Omega}\right)^{ee\to ee} \approx \left(\frac{d\sigma}{d\Omega}\right)^{ee\to ee}_{\rm QED} + \frac{1}{M^2}\left\{\frac{9}{4}\frac{\Gamma_{ee}^2}{\Gamma M}\left(1+\cos^2\theta\right)(1+\delta_{\rm sf})\,\mathrm{Im}\,\mathcal{F} - \frac{3\alpha}{2}\frac{\Gamma_{ee}}{M}\left[\left(1+\cos^2\theta\right) - \frac{(1+\cos\theta)^2}{(1-\cos\theta)}\right]\mathrm{Re}\,\mathcal{F}\right\}. \tag{5}$$

The goal of this analysis is a measurement of $\Gamma_{ee}\times\Gamma_{ee}/\Gamma$ and $\Gamma_{ee}\times\Gamma_{\mu\mu}/\Gamma$ contained in the resonant terms. The precision of these terms in formulae (1) and (5) is better than 0.2%. It was estimated by numerical calculations beyond the soft photon approximation according to Ref. [15]. Although the interference terms could allow one a direct measurement of Γ_{ee} ($e^+e^-\to e^+e^-$) and $\sqrt{\Gamma_{ee}\Gamma_{\mu\mu}}$ ($e^+e^-\to\mu^+\mu^-$), in our case we are limited by the statistical accuracy and theoretical uncertainty.

To compare experimental data with the theoretical cross sections (1) and (5), it is necessary to perform their convolution with a distribution of the total beam energy which is assumed to be Gaussian with an energy spread σ_W:

$$\rho(W) = \frac{1}{\sqrt{2\pi}\sigma_W}\exp\left(-\frac{(W-W_0)^2}{2\sigma_W^2}\right),$$

where W_0 is an average c.m. collision energy.

Since the energy spread $\sigma_W \simeq 0.7$ MeV is much larger than the intrinsic width of the J/ψ meson, the uncertainty of the cross section due to the knowledge of the latter is suppressed. We use the value $\Gamma \simeq 0.093$ MeV [5].

For simulating the nonresonant contribution $\sigma_{\rm QED}$ we use the calculations of [17,18] as implemented in two independent generators BHWIDE [19] and MCGPJ [20].

The resonant and interference cross sections were simulated using simple generators with proper angular distributions. In this case the initial state radiative corrections are already taken into account by the expressions (1) and (5). These formulae implicitly involve the branching ratios $\Gamma_{\ell\ell}/\Gamma = \mathcal{B}_{\ell\ell(n\gamma)}$ with the arbitrary number of soft photons emitted. Actual event selection criteria cannot be 100% efficient for events with additional photons, therefore the final state radiation must be simulated explicitly. This was done using the PHOTOS package [21].

5. Data analysis

In our analysis we employed the simplest selection criteria that ensured sufficient suppression of multihadron events and the cosmic-ray background. The following requirements were imposed for $e^+e^-\to e^+e^-$ events selection:

1. An event should have exactly two oppositely charged tracks, each originating from the beam intersection region, having a continuation in the calorimeter, and lying in the range of angles between the particle and beam axis from 30° to 150°.
2. The energy deposited in the calorimeter for each particle should be higher than 0.7 GeV, and the sum of the energies of the two particles should be higher than 2 GeV.
3. The energy deposited in the calorimeter and not associated with the two particles considered should not exceed 5% of the total energy deposition.
4. The angle between selected particles should be larger than 140° and acoplanarity less than 40°.

Requirements for selecting $e^+e^-\to\mu^+\mu^-$ events are:

1. The same as tracking criteria for $e^+e^-\to e^+e^-$.
2. The energy deposited in the calorimeter for each particle should be higher than 60 MeV and less than 500 MeV, and the sum of the energies of the two particles should not be higher than 750 MeV.
3. The energy deposited in the calorimeter and not associated with the two particles considered should not exceed 30% of the total energy deposition.
4. The angle between selected particles should be larger than 170° and acoplanarity less than 15°.
5. The momentum for each particle should be higher than 500 MeV/c, and the sum of the momenta of the two particles should be higher than 2 GeV/c.
6. There is at least one time measurement in the time-of-flight system. The uncorrected measured time should be within the [−3.75–10.0] ns range from the beam intersection time.

Fig. 3 shows the distribution of selected $e^+e^-\to e^+e^-$ events with respect to the electron scattering angle. The displayed points represent the experimental values, while the histograms correspond to the simulation. At small angles Bhabha scattering prevails, while at large angles events of resonance decay are dominant. The interference effect is not shown since the presented data correspond to the J/ψ peak, where the interference vanishes.

In order to measure the resonance parameters, the set of events was divided into ten equal angular intervals from 40° to 140°. At the i-th energy point E_i and the j-th angular interval θ_j, the expected number of $e^+e^-\to e^+e^-$ events was parameterized as

$$N_{\rm exp}(E_i,\theta_j) = \mathcal{R}_{\mathcal{L}} \times \mathcal{L}(E_i) \times \big(\sigma^{\rm theor}_{\rm res}(E_i,\theta_j)\cdot\varepsilon^{\rm sim}_{\rm res}(E_i,\theta_j) + \sigma^{\rm theor}_{\rm inter}(E_i,\theta_j)\cdot\varepsilon^{\rm sim}_{\rm inter}(E_i,\theta_j) + \sigma^{\rm sim}_{\rm Bhabha}(E_i,\theta_j)\cdot\varepsilon^{\rm sim}_{\rm Bhabha}(E_i,\theta_j)\big), \quad (6)$$

where $\mathcal{L}(E_i)$ is the integrated luminosity measured by the luminosity monitor at the i-th energy point; $\sigma^{\rm theor}_{\rm res}$, $\sigma^{\rm theor}_{\rm inter}$ and $\sigma^{\rm theor}_{\rm Bhabha}$ are the theoretical cross sections for resonance, interference and Bhabha contributions, respectively. $\varepsilon^{\rm sim}_{\rm res}$, $\varepsilon^{\rm sim}_{\rm inter}$ and $\varepsilon^{\rm sim}_{\rm Bhabha}$ are detector efficiencies obtained from simulation. The efficiencies differ mainly due to difference in radiative corrections. Unlike the Bhabha process, the initial state radiation for the narrow resonance production is strongly suppressed, thus the events are more collinear.

In this formula the following free parameters were used:

1. the product $\Gamma_{ee}\times\Gamma_{ee}/\Gamma$, which determines the magnitude of the resonance signal;
2. the electron width Γ_{ee}, which specifies the amplitude of the interference wave;
3. the coefficient $\mathcal{R}_{\mathcal{L}}$, which provides the absolute calibration of the luminosity monitor.

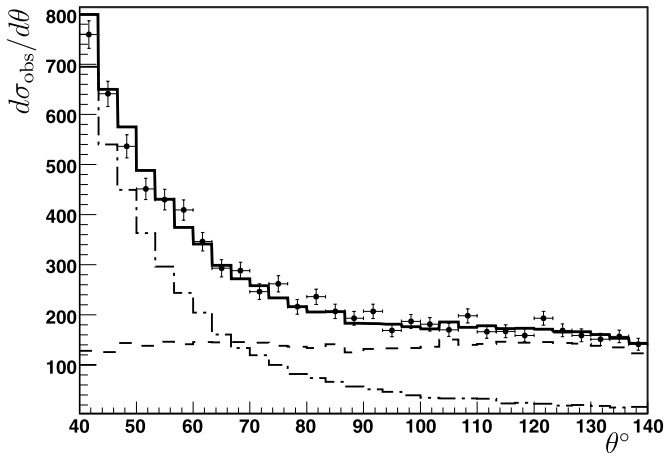

Fig. 3. Cross section of the process $e^+e^-\to e^+e^-$ as a function of the electron scattering angle at the J/ψ peak. The points represent experimental data. The histograms correspond to a simulation: the dashed line represents the contribution of the J/ψ resonance, the dashed and dotted line represents the contribution of Bhabha scattering and the solid-line histogram is the sum of the first two.

We note that the coefficient $\mathcal{R}_{\mathcal{L}}$ partially takes into account a possible difference between the actual detection efficiency and simulation in the case where this difference does not depend on the scattering angle or the beam energy (or the data taking time), thus a substantial cancellation of errors occurs.

The Γ_{ee} value obtained from the fit to the data has large statistical and systematic uncertainties caused by the smallness of the interference effect and the low accuracy of theoretical evaluation.

Fig. 4 shows our fits to the data for four angular bins. For this fit $\chi^2/{\rm ndf} = 53.7/41$ taking into account only the statistical errors and $\chi^2/{\rm ndf}\simeq 40.5/41$ after converting the energy determination uncertainty to the cross section error.

The combined fit in ten equal bins from 40° to 140° produces the following basic result:

$$\Gamma_{ee}\times\Gamma_{ee}/\Gamma = 0.3323\pm 0.0064({\rm stat.})\ {\rm keV},$$
$$\mathcal{R}_{\mathcal{L}} = 93.4\pm 0.7({\rm stat.})\,\%,$$
$$\Gamma_{ee} = 5.7\pm 0.6({\rm stat.})\ {\rm keV}. \quad (7)$$

Due to different angular distributions for Bhabha scattering and resonance events, subdivision of the data into several angular bins reduces the statistical error for $\Gamma_{ee}\times\Gamma_{ee}/\Gamma$ by 40–50%. Here Γ_{ee} has a statistical error of about 10% and agrees with the world average value. The same value can be obtained with a much higher precision using $\Gamma_{\ell\ell}\times\Gamma_{\ell\ell}/\Gamma$ and an independent measurement of the branching ratio $J/\psi\to\ell^+\ell^-$.

Similarly to (6), the expected number of $e^+e^-\to\mu^+\mu^-$ events was parameterized in the form:

$$N_{\rm exp}(E_i) = \mathcal{R}_{\mathcal{L}}\times\mathcal{L}(E_i)\times\big(\sigma^{\rm theor}_{\rm res}(E_i)\cdot\varepsilon^{\rm sim}_{\rm res}(E_i) + \sigma^{\rm theor}_{\rm inter}(E_i)\cdot\varepsilon^{\rm sim}_{\rm inter}(E_i) + \sigma^{\rm theor}_{\rm bg}(E_i)\cdot\varepsilon^{\rm sim}_{\rm bg}(E_i)\big) + F_{\rm cosmic}\times T_i, \quad (8)$$

with the same meaning of $\mathcal{R}_{\mathcal{L}}$ and $\mathcal{L}(E_i)$ as in (6). $\mathcal{L}(E_i)$ is multiplied by the sum of the products of theoretical cross sections for resonance, interference and QED background and detection efficiencies as obtained from simulated data. $\mathcal{R}_{\mathcal{L}}$ was fixed from the result (7) and T_i is the live data taking time. Unlike (6), there is only one angular bin from 40° to 140°.

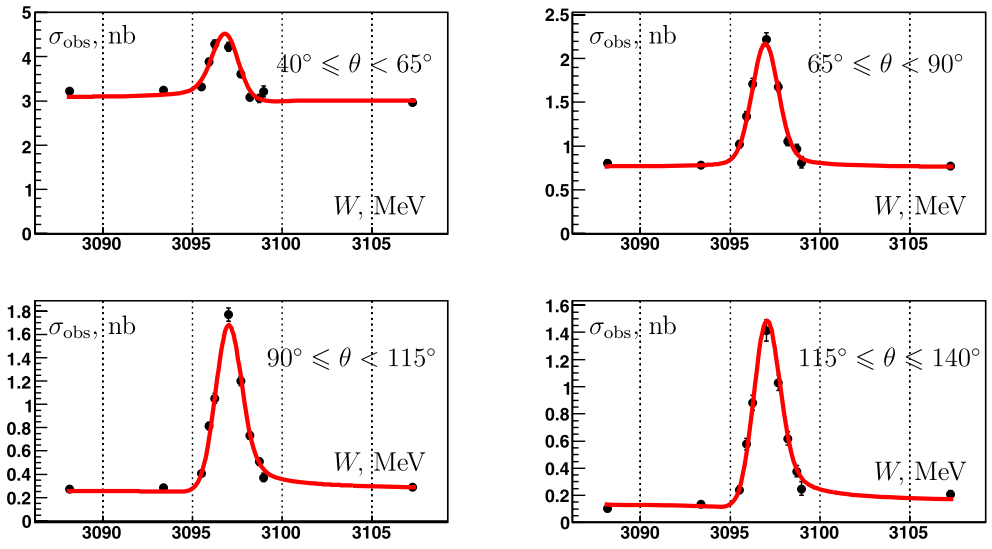

Fig. 4. Fits to experimental data for the process $e^+e^-\to e^+e^-$ in the J/ψ energy range for four angular ranges.

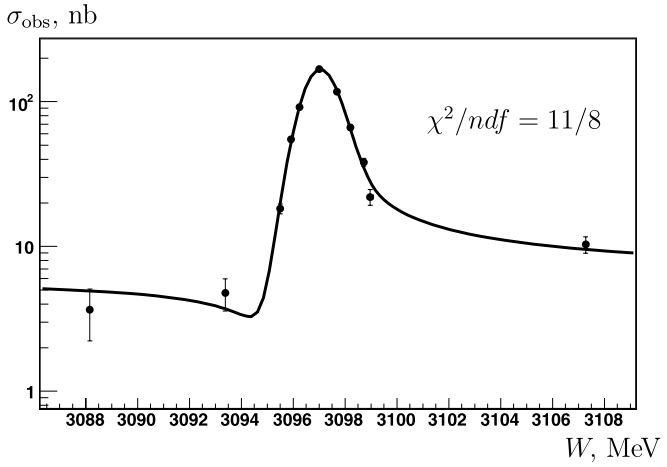

Fig. 5. Fit to experimental data for $e^+e^- \to \mu^+\mu^-$ process in the J/ψ energy range.

The following free parameters were used:

1. the product $\Gamma_{ee} \times \Gamma_{\mu\mu}/\Gamma$, which determines the magnitude of the resonance signal;
2. the square root of electron and muon widths $\sqrt{\Gamma_{ee}\Gamma_{\mu\mu}}$, which specifies the amplitude of the interference wave;
3. the rate of cosmic events, $F_{\rm cosmic}$, that passed the selection criteria for the $e^+e^- \to \mu^+\mu^-$ events.

Due to variations of luminosity during the experiment it is possible to separate the contribution of cosmic events ($F_{\rm cosmic} \cdot T_i$) from that of the nonresonant background ($\sigma_{\rm bg}^{\rm theor}(E_i) \cdot \varepsilon_{\rm bg}^{\rm sim}(E_i) \cdot \mathcal{L}(E_i)$).

Fig. 5 shows our fit to the $e^+e^- \to \mu^+\mu^-$ data. It yields the following result:

$$\Gamma_{ee} \times \Gamma_{\mu\mu}/\Gamma = 0.3318 \pm 0.0052(\text{stat.})\ \text{keV},$$
$$\sqrt{\Gamma_{ee} \times \Gamma_{\mu\mu}} = 5.6 \pm 0.7(\text{stat.})\ \text{keV}. \quad (9)$$

As can be seen from (9), the statistical error of $\Gamma_{ee} \times \Gamma_{\mu\mu}/\Gamma$ is about 1.6%.

6. Discussion of systematic uncertainties

The most significant systematic uncertainties in the $\Gamma_{ee} \times \Gamma_{ee}/\Gamma$ and $\Gamma_{ee} \times \Gamma_{\mu\mu}/\Gamma$ measurements are listed in Tables 1 and 2, respectively. A few dominant sources of uncertainty are briefly described below.

A rather large uncertainty of 0.8% common for the electron and muon channels is due to the luminosity monitor instability. It was estimated from comparing the results obtained using the on-line luminosity of the single bremsstrahlung monitor and the off-line luminosity measured by the e^+e^- scattering in the endcap calorimeter.

The essential source of uncertainty is an imperfection of the detector response simulation resulting in the errors in the trigger and offline event selection efficiencies.

To correct the offline event selection efficiency, two high-purity control samples of e^+e^- events were prepared. The first sample selected using the LKr-calorimeter data only was employed to determine the tracking system efficiency, the second sample obtained using mostly the tracking system data allows one to check calorimeter related cuts. Each sample contains about 70% of all events used in the analysis. The same analysis was performed with simulated data. The corrections already taken into account in (7) were

Table 1
Systematic uncertainties in $\Gamma_{ee} \times \Gamma_{ee}/\Gamma$.

Systematic uncertainty source	Error, %
Luminosity monitor instability	0.8
Offline event selection	0.7
Trigger efficiency	0.5
Energy spread accuracy	0.2
Beam energy measurement (10–30 keV)	0.3
Fiducial volume cut	0.2
Calculation of radiative corrections	0.2
Cross section for Bhabha (MC generators)	0.4
Final state radiation (PHOTOS)	0.4
Background from J/ψ decays	0.2
Fitting procedure	0.2
Total	1.4

Table 2
Systematic uncertainties in $\Gamma_{ee} \times \Gamma_{\mu\mu}/\Gamma$.

Systematic uncertainty source	Error, %
Luminosity monitor instability	0.8
Absolute luminosity calibration by e^+e^- data	1.2
Trigger efficiency	0.5
Energy spread accuracy	0.4
Beam energy measurement (10–30 keV)	0.5
Fiducial volume cut	0.2
Calculation of radiative corrections	0.2
Final state radiation (PHOTOS)	0.5
Nonresonant background	0.1
Background from J/ψ decays	0.6
Total	1.9

$$\delta\Gamma_{ee} \times \Gamma_{ee}/\Gamma = 0.8 \pm 0.6(\text{stat.}) \pm 0.4(\text{syst.})\%,$$
$$\delta\mathcal{R}_{\mathcal{L}} = 1.7 \pm 0.5(\text{stat.}) \pm 0.5(\text{syst.})\%. \quad (10)$$

The statistical error of the efficiency determination is approximately three times less than that of the final result due to the binomial distribution in the number of lost events. The residual systematic error is due to an incomplete event sample employed for the correction and the efficiency difference for the resonance decays and the continuum events. The variation of $\mathcal{R}_{\mathcal{L}}$ is greater than that of the main result illustrating the cancellation of uncertainties mentioned in Section 5.

Three contributions dominate the trigger efficiency uncertainty. The inefficiency of the time-of-flight counters used in the first level trigger was studied using the cosmic ray events and equals 0.3%. The second contribution comes from the cut on the number of the vertex detector tubes hit in the event. It was used in the software trigger level for the machine background suppression. Some fraction of events was accepted unconditionally to check the cut. The third contribution is due to the veto from the CsI crystals nearest to the beam line. It is negligible for the resonance decays and reaches 0.4% for continuum events for which the initial state radiation is not suppressed. The quoted value was obtained varying the threshold in the event filter within its uncertainty. The accidental signal–background coincidences were taken into account by the veto rate with much better accuracy.

The uncertainty of the theoretical Bhabha cross section was estimated comparing the results obtained with the BHWIDE [19] and MCGPJ [20] event generators. It agrees with the accuracies of the generators quoted by the authors.

The dominant uncertainty of the $\Gamma_{ee} \times \Gamma_{\mu\mu}/\Gamma$ result is associated with the absolute luminosity calibration done in the e^+e^--channel. It includes the accuracy of the Bhabha event generators, the statistical error of $\mathcal{R}_{\mathcal{L}}$ from (7) and the residual efficiency difference for e^+e^- and $\mu^+\mu^-$ events after a correction using simulated data.

To determine this residual difference and make a proper correction, samples of real and simulated quasi-collinear events were selected using an alternative track reconstruction code finding a single track with a kink at the point of the closest approach to the beam line. Then the standard analysis procedure was performed for these samples yielding the double ratio

$$\left(\frac{\varepsilon^{\rm exp}_{\mu\mu}}{\varepsilon^{\rm sim}_{\mu\mu}}\right)\Big/\left(\frac{\varepsilon^{\rm exp}_{ee}}{\varepsilon^{\rm sim}_{ee}}\right) = 1.005 \pm 0.005(\text{stat.}) \pm 0.008(\text{syst.}). \qquad (11)$$

The sample selected contains about 80% and 50% of all $\mu^+\mu^-$ and e^+e^- events, respectively. The systematic error of the ratio reflects the incompleteness of the samples.

The trigger veto uncertainty is the same as for $J/\psi \to e^+e^-$ decay.

The background for $J/\psi \to \mu^+\mu^-$ decay from hadronic decays of J/ψ was estimated with the help of the muon system. It contributes $1.5 \pm 0.6\%$ to the selected $\mu^+\mu^-$ events. The estimation agrees with the simulation results. This correction as well as the correction (11) have already been taken into account in the $\Gamma_{ee} \times \Gamma_{\mu\mu}/\Gamma$ result (9).

Due to the high precision in the energy determination by the resonant depolarization method [22], the corresponding errors (peak position, energy spread, and energy at a point) are relatively small.

In calculating the cross section for resonance production with formulae (1) and (5) we used the PDG value of the total width Γ from [5]. Its error is about 2%, which gives a $\sim 0.05\%$ contribution to the error in our result.

The fiducial volume cut $40^\circ < \theta < 140^\circ$ was applied using the tracking system and the strip system of the LKr calorimeter. The difference of results provides a conservative uncertainty estimate.

All other uncertainties are rather clear. More detail can be found in [23].

All the uncertainties for $\Gamma_{ee} \times \Gamma_{ee}/\Gamma$ added in quadrature yield a systematic error of 1.4%. All uncertainties for $\Gamma_{ee} \times \Gamma_{\mu\mu}/\Gamma$ added in quadrature yield a systematic error of 1.9%.

7. Results and conclusion

The new measurement of the $\Gamma_{ee} \times \Gamma_{ee}/\Gamma$ and $\Gamma_{ee} \times \Gamma_{\mu\mu}/\Gamma$ has been performed at the VEPP-4M collider using the KEDR detector. The following results have been obtained:

$$\Gamma_{ee} \times \Gamma_{ee}/\Gamma = 0.3323 \pm 0.0064(\text{stat.}) \pm 0.0048(\text{syst.})\ \text{keV},$$

$$\Gamma_{ee} \times \Gamma_{\mu\mu}/\Gamma = 0.3318 \pm 0.0052(\text{stat.}) \pm 0.0063(\text{syst.})\ \text{keV}.$$

Previously, $\Gamma_{ee} \times \Gamma_{ee}/\Gamma$ was measured in the DASP experiment in 1979 [24] with a precision of about 6%. The result obtained in the present study improves the accuracy by a factor greater than two. The most precise previous measurements of $\Gamma_{ee} \times \Gamma_{\mu\mu}/\Gamma$ were made in the BABAR [25] and CLEO-c [26] experiments, both with the ISR technique.

Fig. 6 shows the comparison of our results with those of the previous experiments. The grey line shows the PDG average and the error for the $\Gamma_{ee} \times \Gamma_{\mu\mu}/\Gamma$ product measurement. The new KEDR results are the most precise. Results are in good agreement with each other and with the world average value of $\Gamma_{ee} \times \Gamma_{\mu\mu}/\Gamma$.

From the direct measurements of the products above one can extract the leptonic and full width of the resonance as well as test leptonic universality. For the former one should calculate the sum of $\Gamma_{ee} \times \Gamma_{ee}/\Gamma$ and $\Gamma_{ee} \times \Gamma_{\mu\mu}/\Gamma$, while for the latter the ratio of these quantities can be used.

While estimating uncertainties of $\Gamma_{ee} \times (\Gamma_{ee} + \Gamma_{\mu\mu})/\Gamma$ and $\Gamma_{ee}/\Gamma_{\mu\mu}$ correlations between $\Gamma_{ee} \times \Gamma_{ee}/\Gamma$ and $\Gamma_{ee} \times \Gamma_{\mu\mu}/\Gamma$ systematic errors were taken into account:

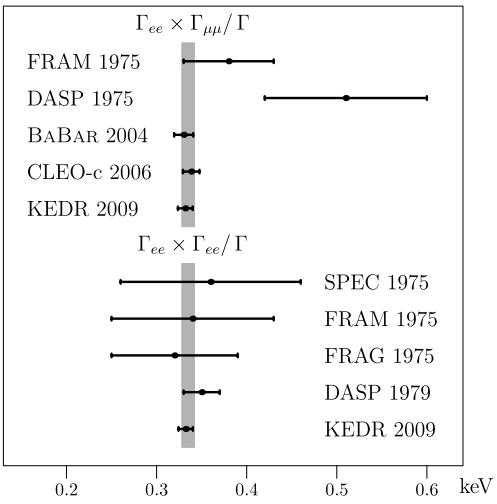

Fig. 6. Comparison of $\Gamma_{ee} \times \Gamma_{ee}/\Gamma$ and $\Gamma_{ee} \times \Gamma_{\mu\mu}/\Gamma$ measured in different experiments mentioned in [5] with KEDR 2009 results. The grey strip is for the world average $\Gamma_{ee} \times \Gamma_{\mu\mu}/\Gamma$ value.

$$\Gamma_{ee} \times (\Gamma_{ee} + \Gamma_{\mu\mu})/\Gamma = 0.6641 \pm 0.0082(\text{stat.}) \pm 0.0100(\text{syst.})\ \text{keV},$$

$$\Gamma_{ee}/\Gamma_{\mu\mu} = 1.002 \pm 0.021(\text{stat.}) \pm 0.013(\text{syst.}).$$

In contrast to the $\Gamma_{ee} \times \Gamma_{ee}/\Gamma$ and $\Gamma_{ee} \times \Gamma_{\mu\mu}/\Gamma$ values, the ratio $\Gamma_{ee}/\Gamma_{\mu\mu}$ is not sensitive to the absolute luminosity calibration. Therefore, the $\mathcal{R}_{\mathcal{L}}$ parameter has been fixed in the fit and the relative statistical uncertainty of the $\Gamma_{ee}/\Gamma_{\mu\mu}$ value is less than that of $\Gamma_{ee} \times (\Gamma_{ee} + \Gamma_{\mu\mu})/\Gamma$.

With the assumption of leptonic universality and using independent data on the branching fraction $\mathcal{B}(J/\psi \to e^+e^-) = (5.94 \pm 0.06)\%$ [5], the leptonic and total widths of the J/ψ meson were determined:

$$\Gamma_{\ell\ell} = 5.59 \pm 0.12\ \text{keV},$$

$$\Gamma = 94.1 \pm 2.7\ \text{keV}.$$

These results are in good agreement with the world average [5] and with the results from the BABAR [25] and CLEO-c [26] experiments.

Acknowledgements

We greatly appreciate the efforts of the staff of VEPP-4M to provide good operation of the complex and the staff of experimental laboratories for the permanent support in preparing and performing this experiment. The authors are grateful to E.A. Kuraev and V.S. Fadin for a discussion of various problems related to theoretical cross section representation.

This work was partially supported by the Russian Foundation for Basic Research, Grant 08-02-00258 and RF Presidential Grant for Scientific Schools NSh-5655.2008.2.

References

[1] A.M. Badalian, I.V. Danilkin, Phys. Atom. Nucl. 72 (2009) 1206.
[2] O. Lakhina, E.S. Swanson, Phys. Rev. D 74 (2006) 014012.
[3] J.J. Dudek, R.G. Edwards, D.G. Richards, Phys. Rev. D 73 (2006) 074507.
[4] N. Brambilla, et al., CERN Yellow Report, CERN-2005-005, arXiv:hep-ph/0412158.
[5] Particle Data Group, C. Amsler, et al., Phys. Lett. B 667 (2008) 1.
[6] V. Anashin, et al., Stockholm 1998, EPAC 98*, 400 (1998), Prepared for 6th European Particle Accelerator Conference (EPAC 98), Stockholm, Sweden, 22–26 June 1998.

[7] A.D. Bukin, et al., Absolute calibration of beam energy in the storage ring. Phi-meson mass measurement, IYF-75-64.
[8] A.N. Skrinsky, Y.M. Shatunov, Sov. Phys. Usp. 32 (1989) 548.
[9] OLYA Collaboration, A.S. Artamonov, et al., Phys. Lett. B 474 (2000) 427.
[10] KEDR Collaboration, V.M. Aulchenko, et al., Phys. Lett. B 573 (2003) 63.
[11] R. Klein, R. Thornagel, G. Ulm, T. Mayer, P. Kuske, Nucl. Instrum. Meth. A 384 (1997) 293.
[12] R. Klein, et al., Nucl. Instrum. Meth. A 486 (2002) 545.
[13] V.V. Anashin, et al., Nucl. Instrum. Meth. A 478 (2002) 420.
[14] Y.I. Asimov, et al., Pis'ma Zh. Eksp. Teor. Fiz. 21 (1975) 378, JETP Lett. 21 (1975) 172.
[15] E.A. Kuraev, V.S. Fadin, Sov. J. Nucl. Phys. 41 (1985) 466.
[16] K.Y. Todyshev, arXiv:0902.4100, 2009.
[17] W. Beenakker, F.A. Berends, S.C. van der Marck, Nucl. Phys. B 349 (1991) 323.
[18] A.B. Arbuzov, et al., JHEP 9710 (1997) 001.
[19] S. Jadach, W. Płaczek, B.F.L. Ward, Phys. Lett. B 390 (1997) 298, UTHEP-95-1001.
[20] A.B. Arbuzov, G.V. Fedotovich, F.V. Ignatov, E.A. Kuraev, A.L. Sibidanov, Eur. Phys. J. C 46 (2006) 689.
[21] E. Barberio, Z. Was, Comput. Phys. Commun. 79 (1994) 291.
[22] V.V. Anashin, et al., JETP Lett. 85 (2007) 347.
[23] V.V. Anashin, et al., Budker INP 2009-9 (in Russian).
[24] DASP Collaboration, R. Brandelik, et al., Z. Phys. C 1 (1979) 233.
[25] BaBar Collaboration, B. Aubert, et al., Phys. Rev. D 69 (2004) 011103.
[26] CLEO Collaboration, G.S. Adams, et al., Phys. Rev. D 73 (2006) 051103.